Solvent Optimization Studies for a New EURO-GANEX Process with 2,2'-Oxybis(*N,N*-di-*n*-decylpropanamide) (mTDDGA) and Its Radiolysis Products

Bart Verlinden, Andreas Wilden, Karen Van Hecke, Richard J. M. Egberink, Jurriaan Huskens, Willem Verboom, Michelle Hupert, Patrik Weßling, Andreas Geist, Petra J. Panak, Rainier Hermans, Marc Verwerft, Giuseppe Modolo, Koen Binnemans & Thomas Cardinaels

Taylor & Francis
Taylor & Francis Group

Solvent Optimization Studies for a New EURO-GANEX Process with 2,2'-Oxybis(*N,N*-di-*n*-decylpropanamide) (mTDDGA) and Its Radiolysis Products

Bart Verlinden [a,b], Andreas Wilden [c], Karen Van Hecke [a],
Richard J. M. Egberink [d], Jurriaan Huskens [d], Willem Verboom [d],
Michelle Hupert [e], Patrik Weßling [f,g], Andreas Geist [f], Petra J. Panak [f,g],
Rainier Hermans [a,h], Marc Verwerft [a], Giuseppe Modolo [c], Koen Binnemans [b],
and Thomas Cardinaels [a,b]

aBelgian Nuclear Research Centre (SCK CEN), Institute for Nuclear Materials Science, Mol, Belgium;
bDepartment of Chemistry, KU Leuven, Leuven, Belgium; cInstitut für Energie- und Klimaforschung -
Nukleare Entsorgung und Reaktorsicherheit- (IEK-6), Forschungszentrum Jülich GmbH, Jülich, Germany;
dMolecular Nanofabrication group, Department of Molecules & Materials, Mesa+ Institute, University of
Twente, Enschede, The Netherlands; eZentralinstitut für Engineering, Elektronik und Analytik (ZEA-3),
Forschungszentrum Jülich GmbH, Jülich, Germany; fInstitute for Nuclear Waste Disposal (INE), Karlsruhe
Institute of Technology (KIT), Karlsruhe, Germany; gInstitut für Physikalische Chemie, Ruprecht-Karls-
Universität Heidelberg, Heidelberg, Germany; hFaculteit Industriële Ingenieurswetenschappen,
UHasselt – KU Leuven, Diepenbeek, Belgium

ABSTRACT

The diglycolamide 2,2'-oxybis(*N,N*-di-*n*-decylpropanamide) (mTDDGA) is being studied as an extractant for actinides and lanthanides in the European Grouped Actinide Extraction (EURO-GANEX) process. The aim is the development of a more simplified process using a single extractant instead of a mixture of extractants used in the current EURO-GANEX process. This work presents solvent optimization studies of mTDDGA, with regards to the extraction characteristics of the different diastereomers of mTDGA and of mixed diastereomer solutions. Also radiolysis behavior has been studied by irradiation of solvent extraction systems in a gamma irradiation facility using ^{60}Co. The availability of irradiated organic solutions made it possible to gain valuable insights into the plutonium loading capacity after gamma-irradiation of the solvent up to 445 kGy and to quantify degradation compounds. Solvent extraction characteristic of the major degradation compounds themselves were determined. Like other methylated diglycolamides, we found a remarkable difference in extraction of up to two orders of magnitude between the two diastereomers. High plutonium loading (36 g L^{-1}) is feasible using this single extractant, even after absorbing a dose of 445 kGy. This remarkable observation is possibly promoted by the presence of the main degradation compound which extracts plutonium verywell.

CONTACT Karen Van Hecke   karen.van.hecke@sckcen.be   Belgian Nuclear Research Centre (SCK CEN), Institute for Nuclear Materials Science, Boeretang 200, Mol 2400, Belgium

Supplemental data for this article can be accessed online at https://doi.org/10.1080/07366299.2022.2125151.

Introduction

Nuclear fission reactions have been used for electricity production for the past 70 years. Despite the advantage of low carbon dioxide emissions, there is also the inevitable production of highly radioactive waste. This irradiated nuclear fuel needs isolation from the biosphere for hundreds of thousands of years. Deep geological repositories are therefore studied in many countries as the preferred disposal option. The required space in repositories is highly dependent on the heat production. Radiotoxicity and heat emission on the long term (after a few hundred years) originate mainly from the decay of actinides such as Pu, Np, Am, and Cm.[1] For this reason, separation of these elements from used nuclear fuel and, in case of a scenario involving GEN IV nuclear reactors, reduction of the total inventory of these long-lived isotopes, would improve resource efficiency (the repository in this case being considered a scarce resource).[1–6]

The Grouped Actinide Extraction (GANEX) process concept is based on the strategy to extract the actinides together and avoid separating a pure Pu stream, which would raise concerns towards proliferation.[7,8] The bulk amount of U in the dissolved used nuclear fuel is extracted with 1 mol L^{-1} N,N-di(ethyl-2-hexyl)isobutyramide (DEHiBA) in a first cycle (GANEX-1).[9] The following process then separates the actinides (Pu, Np, Am, Cm, and remaining small amounts of U) from fission and corrosion products. For this second cycle, the CEA GANEX process made use of 0.6 mol L^{-1} N,N'-dimethyl-N,N'-dioctyl-2(2-hexyloxyethyl)-malonamide (DMDOHEMA) and 0.3 mol L^{-1} di(2-ethylhexyl)phosphoric acid (HDEHP) for the coextraction of actinides and lanthanides. This was followed by an actinide selective stripping with N-(2-hydroxyethyl)-ethylenediamin-N,N',N'-triacetic acid (HEDTA) and citric acid.[10,11] Both of these cycles, initially developed by the CEA, were demonstrated on irradiated uranium oxide fuel solutions.[9,11]

During previous European projects (ACSEPT[12,13] and SACSESS[14,15]) further improvements of this separation strategy were exploited, resulting in the development and demonstration of the EURO-GANEX process. Here, the separation for the second cycle is achieved by co-extraction of actinides and lanthanides followed by an actinide-selective stripping. A solvent of 0.2 mol L^{-1} N,N,N',N'-tetra-n-octyl diglycolamide (TODGA) and 0.5 mol L^{-1} N,N'-dimethyl-N,N'-dioctylhexylethoxy-malonamide (DMDOHEMA) in Exxsol D80 aliphatic diluent was used for the actinide and lanthanide extraction.[16,17] The hydrophilic N-donor ligand 2,6-bis(5,6-di(sulfophenyl)-1,2,4-triazin-3-yl)pyridine (SO_3-Ph-BTP) was used in combination with acetohydroxamic acid (AHA) for selectively back-extracting the actinides from the loaded solvent. The EURO-GANEX process was demonstrated on an aqueous feed from irradiated fast reactor fuel with a high plutonium content.[18] The solvent, however, has a rather complex formulation with two extractants at

high concentrations, which required the use of CDTA as masking agent to reduce fission product co-extraction.[18,19] A more simplified solvent would be preferable considering simplified solvent formulation, but also for solvent recycling. Since both extractants will be degraded by ionizing radiation, the resulting mixture of degradation compounds will be more complex.

Within the GENIORS project an optimized solvent formulation for the EURO-GANEX process was studied. 2,2'-Oxybis(*N,N*-di-*n*-decylpropana-mide) (mTDDGA) was suggested as a single extractant to replace the combination of TODGA and DMDOHEMA.[20] Avoiding the use of DMDOHEMA would be advantageous, as it caused co-extraction of certain fission products.[20] However, TODGA on its own is not suitable for application on feed solutions containing high concentrations of Pu. During initial EURO-GANEX optimization studies, different TODGA solvents were tested and TODGA alone was found to be prone to third-phase formation when using ≥ 5 g L^{-1} Pu in the feed.[21] For this reason, DMDOHEMA initially had to be included in the EURO-GANEX solvent extraction system.[21] The Pu loading capacity increases for diglycolamides (DGAs) with longer alkyl chains.[21,22] Therefore, the use of a diglycolamide with decyl side chains was proposed.[20] The ligand concentration was also increased to further improve the metal loading capacity. This increase of the diglycolamide concentration on the other hand yields very high metal ion distribution ratios, resulting in unwanted co-extraction of fission products and difficult back-extraction of actinides in the stripping section of a process. Therefore, the backbone of the diglycolamide was methylated to reduce distribution ratios.[20,23,24] The most important ligands for EURO-GANEX are shown in Figure 1.

The double methylated mTDDGA can occur in two different diastereomers, the *R,S* configuration with the methyl groups oriented in the same direction, and the *S,S* or *R,R* configuration with the methyl groups oriented in opposite directions. This seemingly small difference could greatly influence the extractants' complexing capabilities, as this was the case for the analogues TODGA
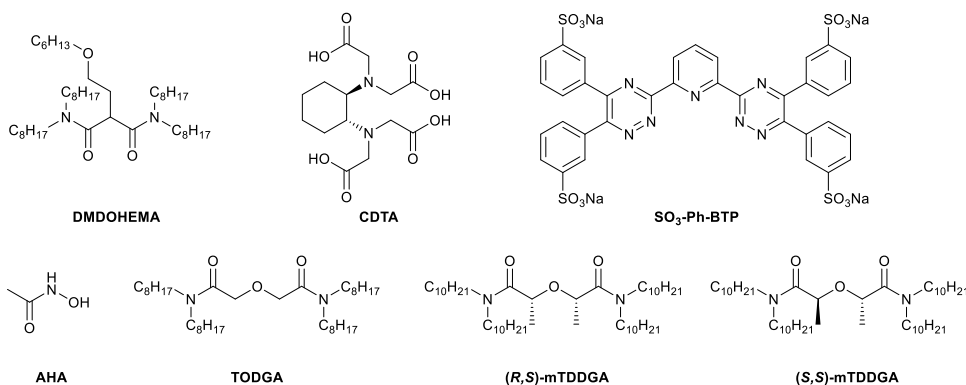

Figure 1. Chemical structures of EURO-GANEX complexants and two diastereomers of mTDDGA.

derivative Me$_2$TODGA; differences of the distribution ratios of up to two orders of magnitude were reported.[25] Computational work in combination with Extended X-ray Absorption Fine Structure (EXAFS) showed that these differences originate from complexation of the nitrates, which was found to be different for the two diastereomers due to the orientation of the methyl groups.[25] Based on these findings, such differences are also be expected for mTDDGA, and reported herein.

The radiolytic stability of the extractants is a key parameter for the evaluation of their usability and long-term performance of separation processes.[26–31] Diglycolamides, such as TODGA, have been subject to many radiolysis studies.[2932–39] In general, the concentration of diglycolamides decreases exponentially as solutions are irradiated. The slope of the natural logarithm of the DGA concentration as a function of dose, the dose constant d, is an easy to use figure of merit for comparison of different DGAs or irradiation conditions.[40] Sugo et al. reported that lower concentrations of TODGA are less stable towards ionizing radiation;[32] the diluent (n-dodecane) sensitizes the molecule. Pulse radiolysis studies indicated that the radiolysis of DGAs is driven by reactions with radical cations of the diluent.[41,42] As the extractants are used in contact with aqueous nitric acid solutions, the influence of this aqueous phase also needs to be considered. Radiolysis of water and nitric acid induce highly reactive radical species such as $^\bullet$OH, $^\bullet$H, NO$_3$$^\bullet$ and molecular species such as H$_2$O$_2$and HNO$_2$possibly causing higher degradation rates.[43–45] On the other hand, nitric acid could have a protective effect, as reported for TODGA by Galán et al.[46] For Me$_2$TODGA, Galán et al. reported a higher stability than for TODGA itself. However, when irradiated in the presence of an aqueous nitric acid solution of 2.5 mol L^{-1}, the observed dose constant (degradation rate) increased from -3.0×10^{-3}kGy^{-1}to -5.3×10^{-3}kGy^{-1}.[37] For single methylated TODGA (MeTODGA), however, dose constants were higher.[37] Calculations showed destabilization of both ether bonds, while Me$_2$TODGA offered steric protection.[47] Main degradation compounds of mTDDGA were identified and found to be similar to the ones reported for other DGAs.[33] Common degradation compounds of diglycolamides resulting from cleavage of the central ether bond are N,N-alkylamides, in some cases with an alcohol group.[37,39,46] It has been known since the 1950's that amides are able to form complexes with (actinide) metal ions.[48,49] Siddall showed in 1960 that for the extraction of actinides and Zr by N,N-dialkylamides, successive alkylations of the α carbon leads to a decrease of extraction of tetravalent metal ions and in a less extent of hexavalent actinides and nitric acid.[48] Small differences in their structure and functional groups strongly affect their extraction behavior. Hubscher-Bruder et al. studied *degradation compounds*(DCs) of methylated TODGA.[39] They synthesized the DCs and used them for quantification in irradiated solvents and for solvent extraction studies with the DCs. For the most abundant DCs in the irradiated samples (up to 1000 kGy), extraction behavior was determined.

In this work, solvent optimization studies of mTDDGA are presented. The extraction behavior of the different diastereomers is presented and the radiolytic stability is evaluated. Degradation compounds are quantified, and the extraction behavior of the main degradation products is studied.

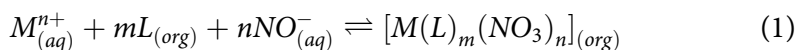## Experimental

Chemicals

Solutions were prepared by weighing the required amount of mTDDGA followed by dilution with n-dodecane (GPR Rectapur purchased from VWR) or Exxsol D80 (ExxonMobil Chemicals). Nitric acid solutions were prepared by dilution of 65% nitric acid (p.a.) purchased from Merck or 68% TraceMetal Grade from Fisher Chemical.

Solvent extraction experiments

Aqueous solutions for solvent extraction were prepared by dissolution of metal nitrate salts in nitric acid and dilution in the appropriate nitric acid concentration to metal concentrations of 10^{-5} mol L^{-1}. The aqueous phases were spiked with ca. 1 kBq each of ^{152}Eu, ^{237}Np (in equilibrium with ^{233}Pa), ^{239}Pu, ^{241}Am and ^{244}Cm (each) before solvent extraction. Batch solvent extraction experiments were conducted in 2 mL vials with 500 μL of each phase. Extraction was conducted at 25°C, 2500 rpm shaking for 1 h using a Vibrax® from IKA, unless mentioned otherwise. Clean phase separation was obtained after 5 minutes centrifugation at 3250 rpm. Then, phases were separated manually using pipettes. If mentioned, pre-equilibration was conducted in the same manner as the described solvent extraction experiments with corresponding aqueous nitric acid solutions. Distribution ratios for radiotracer elements were determined based on measurements by alpha and gamma spectrometry. For gamma spectrometry (HPGe detector, Canberra), aliquots of 200 μL of each phase were transferred to 2 mL vials for measurement. Peak areas by data analysis with Genie2000 software are converted into count rates using the measurement live-time and used to calculate distribution ratios by dividing the result for the organic phase by the count rate for the aqueous phase. For alpha spectrometry, 10 μL aliquots were transferred to metal plates and fixated by burning with a handheld butane torch. For gamma (using the 59.5 keV γ peak for Am and the 121.8 keV γ peak for ^{152}Eu) and alpha spectrometry, samples were measured until 10,000 counts were reached, except for very low activity samples. Inductively coupled plasma mass spectrometry (NexION2000 type C from PerkinElmer) was used to determine concentrations of the nonradioactive metal ions. Samples were diluted 1 to 100 in 1% HNO_3 for aqueous phases and in 1% HNO_3 and 0.2% Triton X-100 (Sigma

Aldrich) for the organic phases. Generally, using these techniques uncertainty of the determined distribution ratios is determined ≤5% between 0.01 and 100, and ≤20% for the range 0.001–0.01 and 100–1000.

Slope analysis of the distribution ratios as a function of the ligand concentration was conducted based on the following complexation Eq. (1) with metal ion (M) and ligand (L).

$$M^{n+}_{(aq)} + mL_{(org)} + nNO^-_{(aq)} \rightleftharpoons [M(L)_m(NO_3)_n]_{(org)} \qquad (1)$$

When only the ligand concentration is varied, m can be derived from the slope of the linear regression of the logarithm of the distribution ratio as a function of the logarithm of the ligand concentration (Eq. (2)). This value gives an indication of the stoichiometry of the complexation reaction.[50,51]

$$\log(D_M) = m \cdot \log([L]) + \log(K) + n \cdot \log([NO_3^-]) \qquad (2)$$

Gamma irradiation

Gamma irradiation was conducted using the previously validated method using ⁶⁰Co sources at SCK CEN.[52] Red Perspex dosimetry was used to determine dose rates at the exact sample location in the irradiation container to ensure high accuracy of the absorbed doses of the samples. This dosimetric method is based on measuring the discoloration of thin (red) plexiglass plates, which correlates with the absorbed dose which was previously validated for this particular irradiation facility.[52] The average dose rate at the samples' position was 9.44 kGy h^{-1}. Samples were irradiated in contact with air in 4 mL screw cap vials of which screw caps were replaced after irradiation. Before sampling and solvent extraction, all samples were centrifuged to remove any solid precipitate. Organic phases irradiated without aqueous phase did not show any sign of present precipitate, this was only the case for the samples in contact with nitric acid solutions. From two irradiated samples containing precipitate, HPLC-MS samples of the precipitate were prepared. One sample of the precipitate was put on a paper filter, washed with n-dodecane, and dissolved in a small amount of methanol. Another sample was prepared by washing the organic phase with precipitate directly with methanol. This methanol phase was then analyzed with HPLC-MS.

Plutonium loading

Plutonium loading was conducted by dilution of the 68 g L^{-1} Pu(IV) stock solution in 5.85 mol L^{-1} HNO$_3$ to 32 g L^{-1} Pu(IV) in 5 mol L^{-1} HNO$_3$. Samples for ICP-MS analysis were diluted 8×10^6 times. Screw cap vials with 400 μL of the aqueous phase and 400 μL of irradiated 0.5 mol L^{-1} (R,S)-mTDDGA in

Exxsol D80 were shaken for 1 h at 21°C. After centrifugation, samples were taken for analysis. Plutonium in the organic phase was back-extracted by shaking of 0.25 mL of the organic phase to 2.5 mL 4 mol L^{-1} AHA in 0.3 mol L^{-1} HNO$_3$ for 1 hour. After centrifugation, 50 µL of this organic phase was back-extracted a second time with fresh 4 mol L^{-1} AHA solution (500 µL) in 0.3 mol L^{-1} HNO$_3$. Determined Pu concentrations of both back-extractions were used for calculation of the Pu concentration in the organic phase.

Synthesis

Di-*n*-decylamine, *n*-decylamine, propionyl chloride, lactic acid, and silicagel 60 (230–400 mesh) were obtained from Sigma Aldrich and were used without further purification. Pyridine was obtained from Sigma Aldrich and was dried over KOH for at least 7 days before use. 1-(3-Dimethylaminopropyl)-3-ethyl-carbodiimide hydrochloride (EDC•HCl) was obtained from TCI Europe and was rinsed with dry diethyl ether immediately before use. Dry diethyl ether, THF, toluene, dichloromethane and hexane were obtained from Actu-All Chemicals and dispensed with a MBraun MB SPS 800 system. ^{1}H and ^{13}C NMR spectra were recorded on a Bruker Ascend^{TM} 400 MHz NMR spectrometer. HRMS mass spectra were recorded on an Orbitrap LTQ XL mass spectrometer at the University of Münster (Germany).

(2*R*,2'*S*)-2,2'-Oxybis(*N*,*N*-di-*n*-decylpropanamide) ((*R*,*S*)-mTDDGA)

(2*R*,2'*S*)-2,2'-Oxydipropionic acid[25] (5.00 g, 30.8 mmol) and di-*n*-decyla-mine (19.25 g, 64.7 mmol) were dissolved in pyridine (100 mL). EDC•HCl (17.73 g, 92.5 mmol; 3 equiv) was added and the mixture was stirred overnight at room temperature under an argon atmosphere. The solvent was removed by rotary evaporation. The residue was stripped with toluene, hexane and dichloromethane, successively. The residue was taken up in dichloromethane (200 mL) and washed with HCl (2 mol L^{-1}), and water. Drying over MgSO$_4$ and removal of the solvent resulted in a yellow oil, which was purified by column chromatography (SiO$_2$, Et$_2$O/heptane 15/35, later gradually changed into Et$_2$O/heptane 1/1) to give (*R*,*S*)-mTDDGA. Yield 15.7 g (71%) color-less oil.

^{1}H NMR (400 MHz) δ 4.24 (q, 2 H, *J* = 6.5 Hz, C*H*CH$_3$), 3.5–3.4 (m, 2 H, NCH$_2$), 3.25–3.0 (m, 6 H, NCH$_2$), 1.5–1.4 (m, 8 H, NCH$_2$C*H*$_2$), 1.37 (d, *J* = 6.5 Hz, 6 H, CHC*H*$_3$), 1.3–1.1 (m, 56 H), 0.9–0.8 (dt, 12 H, CH$_2$C*H*$_3$); ^{13}C NMR δ 171.85, 71.4, 47.1, 46.1, 31.90, 31.88, 29.63, 29.59, 29.56, 29.46, 29.43, 29.32, 27.6, 27.03, 26.95, 22.67, 19.1, 14.1; ESI-MS *m/z* 721.9 [M+H]+; HRMS: *m/z* = 720.7186, calcd for C$_{46}$H$_{92}$N$_2$O$_3$+ 720.7181.

(2*S*,2'*S*)-2,2'-Oxybis(*N*,*N*-di-*n*-decylpropanamide) ((*S*,*S*)-mTDDGA)

The same procedure (albeit at smaller scale) was used for the preparation of (*S*,*S*)-mTDDGA, starting from (2*S*,2'*S*)-2,2'-oxydipropionic acid.[25] It was

isolated as a colorless oil in 67% yield after column chromatography (SiO_2, Et_2O/heptane 15/35, later gradually changed into Et_2O/heptane 1/1).

^{1}H NMR δ 4.40 (q, 2 H, $J = 6.5$ Hz, C*H*CH$_3$), 3.5–3.15 (m, 8 H, NC*H*$_2$), 1.6–1.5 (m, 8 H, NCH$_2$C*H*$_2$), 1.6–1.5 (62 H, C*H*$_2$and CHC*H*$_3$), 0.9–0.8 (dt, 12 H, CH$_2$C*H*$_3$); ^{13}C NMR δ 171.25, 69.8, 47.2, 46.1, 31.89, 31.88, 29.62, 29.60, 29.56, 29.53, 29.44, 29.41, 29.31, 27.5, 27.1, 26.9, 22.7, 17.8, 14.1; ESI-MS m/z 722.0 [M+H]+; HRMS: $m/z = 720.7184$, calcd for $C_{46}H_{92}N_2O_3+$ 720.7181.

The diastereomeric 3.5:1 mixture of (*R,S*)-mTDDGA and (*S,S*)-mTDDGA was prepared in the same way from the corresponding mixture of 2,2'-oxydipropionic acid.[25]

(2*R*,2'*S*)-*N*,*N*-Di-*n*-decyl-2-((1-(decylamino)-1-oxopropan-2-yl)oxy)propenamide (DC I)

EDC•HCl (1.07 g, 5.61 mmol) was added to a solution of (2*R*,2'*S*)-2-((1-(di-*n*-decylamino)-1-oxopropan-2-yl)oxy)propanoic acid (DC VII; 1.65 g, 3.74 mmol) and *n*-decylamine (0.59 g, 3.74 mmol) in dry pyridine (30 mL) at room temperature. After stirring overnight, the pyridine was removed by a rotary evaporator. The residue was stripped with toluene, hexane, and dichloromethane (each 25 mL), successively. The crude product was dissolved in dichloromethane and washed with water (3×25 mL) to remove EDC residues. Column chromatography (SiO_2, Et_2O/hexane (at first 1:1 (v/v), later changed to 35:15)) yielded 70% of the product.

^{1}H NMR δ 6.63 (bt, 1 H, NH), 4.23 (q, 1 H, $J = 6.5$ Hz, C*H*CH$_3$ C(O)N(CH$_2$)$_2$), 3.77 (q, 1 H, $J = 6.7$ Hz, C*H*CH$_3$C(O)NH), 3.4–3.05 (m, 6 H, NC*H*$_2$), 1.55–1.4 (m, 6 H, NCH$_2$C*H*$_2$), 1.33 (d, 3 H, $J = 7.1$ Hz, CHC*H*$_3$), 1.31 (d, 3 H, $J = 6.3$ Hz, CHC*H*$_3$), 1.3–1.1 (m, 42 H, CH$_2$), 0.81 (t, 3 H, $J = 7.0$ Hz, CH$_3$), 0.81 (t, 6 H, $J = 6.5$ Hz, CH$_3$); ^{13}C NMR δ 173.1, 171.0, 77.2, 75.8, 72.1, 47.3, 46.2, 38.9, 31.88, 31.86, 29.7, 29.57, 29.56, 29.53, 29.50, 29.45, 29.37, 29.31, 29.29, 29.27, 27.5, 26.96, 26.92, 26.90, 22.66, 22.65, 19.2, 18.4, 14.1; HRMS: $m/z = 603.5440$ (M+Na)+, calcd for $C_{36}H_{72}N_2O_3$ Na+ 603.5435.

N,*N*-Di-*n*-decylpropionamide (DC II)

A solution of NaOH (3.36, 84.0 mmol) in water (25 mL) was added at room temperature to a solution of di-*n*-decylamine (5.0 g, 16.8 mmol) in a mixture of THF (30 mL) and ethyl acetate (15 mL). The mixture was cooled to 0°C, and propionyl chloride (1.63 g, 17.6 mmol) was added dropwise. After the addition was complete, the mixture was stirred for 30 minutes, and allowed to come to room temperature. The reaction mixture was concentrated (rotary evaporator) and the residue extracted with diethyl ether (3×25 mL). Washing with HCl (2N, 2×25 mL) and brine (25 mL) followed by drying over MgSO$_4$yielded the product as an almost colorless oil (72%).

^{1}H NMR δ 3.30–3.24 and 3.21–3.15 (m, 4 H, NCH_2), 2.30 (q, 2 H, $J = 8$ Hz, C(O)CH_2CH$_3$), 1.6–1.45 (m, 4 H, NCH$_2$CH_2), 1.35–1.20 (m, 28 H, CH$_2$), 1.13 (t, 3 H, $J = 8$ Hz, C(O)CH$_2$CH_3), 0.9–0.8 (m, 6 H, CH$_2$CH$_2$ CH_3); ^{13}C NMR δ 173.2, 77.2, 47.9, 45.9, 31.91, 31.88, 29.62, 29.57, 29.52, 29.46, 29.38, 29.32, 29.29, 29.1, 27.8, 27.1, 26.9, 26.3, 22.69, 22.68, 14.1, 9.7; HRMS: $m/z = 376.3548$ (M+Na)+, calcd for C$_{23}$H$_{47}$NONa+ 376.3550.

N,N-Di-*n*-decyllactamide (DC III)

The compound was prepared according to the procedure described by Fein and Filachione, starting from pure lactic acid instead of the 80% aqueous solution mentioned in the reference.[53]

^{1}H NMR δ 4.32 (sept, 1 H, C(O)CHCH$_3$), 3.75 (d, 1 H, $J = 7.6$ Hz, OH), 3.55–3.45 (m, 1 H, NCH), 3.20–3.10 (m, 1 H NCH), 3.1–2.95 (m, 2 H, NCH), 1.55–1.4 (m, 4 H, NCH$_2$CH$_2$), 1.25 (d, 3 H, $J = 6.5$ Hz, C(O)CHCH_3), 1.3–1.1 (m, 38 H, CH_2CH$_3$ and CH$_2$CH_3); ^{13}C NMR δ 174.7, 77.2, 64.2, 46.7, 45.8, 31.88, 31.85, 29.56, 29.53, 29.49, 29.37, 29.31, 29.30, 29.26, 28.8, 27.5, 26.9, 26.8, 22.68, 22.67, 21.9, 14.1; HRMS: $m/z = 392.3497$ (M+Na)+, calcd for C$_{23}$H$_{47}$NO$_2$Na+ 392.3499.

(2*R*,2'*S*)-2-((1-(Di-*n*-decylamino)-1-oxopropan-2-yl)oxy)propanoic acid (DC VII)

EDC•HCl (1.77 g, 9.25 mmol) was added to (2*R*,2'*S*)-2,2'-oxydipropionic acid (2.00 g, 12.34 mmol) and di-*n*-decylamine (1.84 g, 6.17 mmol) dissolved in dry pyridine (30 mL) at room temperature. After stirring overnight, the pyridine was removed by rotary evaporator. The residue was stripped with toluene, hexane, and dichloromethane (each 25 mL) successively. The crude product was dissolved in dichloromethane and washed with portions of water (3 × 25 mL) to remove EDC residues. Column chromatography (SiO2, Et$_2$O/hexane (at first 1:1 (v/v), later changed to 35:15)) yielded 58% of the product.

^{1}H NMR δ 9.2 (bs, 1 H COOH), 4.56 (q, 1 H, $J = 6.6$ Hz, CHCH$_3$C(O)N), 4.14 (q, 1 H, $J = 6.8$ Hz, CHCH$_3$COOH), 3.55–3.1 (m, 4 H, NCH_2), 1.65–1.5 (m, 4 H, NCH$_2$CH_2), 1.47 (d, 3 H, $J = 7.1$ Hz, CHCH_3COOH), 1.44 (d, 3 H, $J = 6.8$ Hz, CHCH_3C(O)N), 1.4–1.1 (m, 28 H, CH$_2$), 0.89 (t, 3 H, $J = 7.2$ Hz, CH$_2$CH_3), 0.88 (t, 3 H, $J = 6.5$ Hz, CH$_2$CH_3); ^{13}C NMR δ 176.2, 172.9, 77.2, 72.5, 72.1, 47.2, 46.3, 31.88, 31.86, 29.57, 29.53, 29.50, 29.48, 29.35, 29.30, 29.27, 29.2, 27.4, 26.9, 26.8, 22.67, 22.66, 18.6, 18.2, 14.1; HRMS: $m/z = 464.3707$ (M+Na)+, calcd for C$_{26}$H$_{51}$NO$_4$Na+ 464.3710.

(2*R*,2'*S*)-2,2'-Oxybis(*N*-*n*-decylpropanamide) (DC VIIIb)

EDC•HCl (1.77 g, 9.25 mmol) was added to a solution of (2*R*,2'*S*)-2,2'-oxydipropionic acid[25] (0.96 g, 5.92 mmol) and *n*-decylamine (1.96 g, 12.43 mmol) in dry pyridine (30 mL) at room. After stirring overnight, the pyridine was removed by a rotary evaporator. The residue was stripped with toluene, hexane, and dichloromethane (each 25 mL), successively. The crude product was dissolved in dichloromethane and washed with water (3 × 25 mL) to

remove EDC residues. Column chromatography (SiO$_2$, Et$_2$O/hexane (at first 1:1 (v/v), later changed to 35:15)) gave 76% of the product.

^{1}H NMR δ 6.43 (bt, 2 H NH), 3.93 (q, 2 H, $J = 6.8$ Hz, OCHCH$_3$), 3.4–3.2 (m, 4 H NCH$_2$), 1.6–1.5 (m, 4 H NCH$_2$CH_2), 1.44 (d, 6 H, $J = 6.7$ Hz, OCHCH_3), 1.4–1.2 (m, 28 H, CH$_2$), 0.90 (t, 6 H, CH$_3$); ^{13}C NMR δ 172.1, 77.3, 39.1, 31.9, 29.6, 29.5, 29.29, 29.26, 26.9, 22.7, 19.4, 14.1; HRMS: $m/z = $ 463.3867 (M+Na)+, calcd for C$_{26}$H$_{52}$N$_2$O$_3$Na+ 463.3870.

HPLC-MS analysis

HPLC-ESI-MS/MS was performed with a Qtrap6500 instrument (ABSciex, Darmstadt, Germany) coupled with an Agilent 1260 HPLC consisting of a binary pump system, an autosampler and a thermostatted column (Accucore-150-C4; 100 mm × 4.6 mm; 2.6 μm (Thermo)) compartment at 50°C. The MS-parameters used for all methods were optimized performing a Flow Injection Analysis (FIA) with standards and led to the following settings for all analyses: curtain gas (N$_2$) 40 arbitrary units (au), temperature of the source 350°C, nebulizer gas (N$_2$) 80 au, heater gas (N$_2$) 40 au, and ionspray voltage (IS) 4500 V. Quantitation after HPLC separation was performed using ESI-MS/MS detection in the multiple reaction-monitoring (MRM) mode. All LC-MS/MS data acquisition and processing was carried out using the Software Analyst 1.6.1 (AB Sciex, Darmstadt, Germany). Quantification was performed with the Software Multiquant (AB Sciex, Darmstadt, Germany) for an injection volume 10 μL, the experimental setting for each compound can be found in the supporting information.

Results and discussion

Batch extraction with mTDDGA

Extraction behavior

Initial batch extraction tests with mTDDGA were conducted using a mixture of diastereomers. Figure 2 shows the distribution ratios of actinides and lanthanides as a function of the nitric acid concentration. Distribution ratios of all metal ions increase with increasing HNO$_3$ concentration and reach high D values at the highest HNO$_3$ concentration. Neptunium shows much lower D values, compared to the other actinides, which is probably caused by its speciation. The used Np tracer contains mainly Np(V), and it is known that the Np speciation has a tremendous effect on its extraction.[54] The speciation of Np depends on the nitric acid concentration[55] as well. At a concentration of 4 mol L^{-1} of HNO$_3$, the distribution ratios range from 1.9 for neptunium up to 993 for holmium (in Figure SI- 1). Compared to TODGA, these distribution ratios are much lower, as expected due to the methylation.[23] The distribution
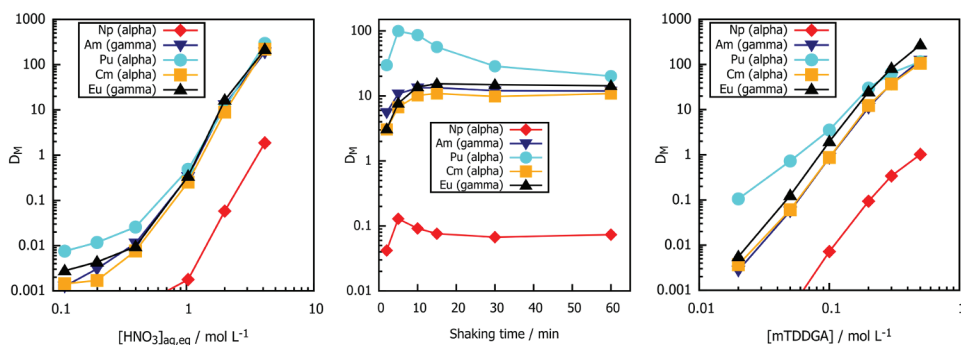
Figure 2. Distribution ratios of radiotracers as a function of the nitric acid concentration. (left) Org.: pre-equilibrated (with an equal volume of corresponding nitric acid solution) 0.5 mol L^{-1} mTDDGA (mixed diastereomers, 3.5:1 (*R,S*):(*S,S*)) in Exxsol D80. Aq.: 10^{-5} mol L^{-1} Ln(III) in nitric acid, tracers: ^{237}Np, ^{239}Pu, ^{241}Am, ^{152}Eu, ^{244}Cm, 500 μl of both phases, shaking 2500 rpm at 25°C for 60 min. Distribution ratios of radiotracers as a function of the shaking time. (center) Org.: 0.5 mol L^{-1} mTDDGA (mixed diastereomers, 3.5:1 (*R,S*):(*S,S*)) in Exxsol D80. Aq.: 10^{-5} mol L^{-1} Ln(III), [Y] in 2 mol L^{-1} HNO$_3$, tracers: ^{237}Np, ^{239}Pu, ^{241}Am, ^{152}Eu, ^{244}Cm, 500 μl of both phases, shaking 2500 rpm at 25°C. Distribution ratios of radiotracers as a function of the mTDDGA concentration. (right) Org. mTDDGA (mixed diastereomers, 3.5:1 (R,S):(S,S)) in Exxsol D80. Aq.: [Ln], [Y] = 10^{-5} mol L^{-1} in 4 mol L^{-1} HNO$_3$, tracers: ^{237}Np, ^{239}Pu, ^{241}Am, ^{152}Eu, ^{244}Cm, O/A ratio = 1, 25°C, 60 min, 2500 rpm.

ratios are also lower (~ one order of magnitude) than the ones reported by Malmbeck et al.[20] The authors did not explicitly report the diastereomeric excess of the mTDDGA they used, but from the description in the paper, it is assumed that they used mainly the (R,S)-mTDDGA diastereomer.[20]

The extraction of actinides and lanthanides (Figure SI- 2) is fast (reaching a plateau after 15 minutes, Figure 2), except for neptunium and plutonium. It is highly probable that the initial oxidation states (+IV for Pu and +V for Np) are not stable under the extraction conditions, as was observed for the initial EURO-GANEX process.[54] For the EURO-GANEX process, it was shown that distribution ratios of Np follow the order D(Np(IV)) >> D(Np(VI)) >> D(Np(V)). The trend for plutonium and neptunium extraction in Figure 2 could therefore be explained by changes in the metal ion speciation (which was not further studied, here).

Table 1. Slopes of the linear fitting of log(d) as a function of log([mtddga]).

Element	Slope
La	2.94 ± 0.19
Nd	3.15 ± 0.12
Eu	3.45 ± 0.12
Gd	3.25 ± 0.11
Ho	3.31 ± 0.11
Np	3.11 ± 0.27
Pu	2.29 ± 0.12
Am	3.43 ± 0.11
Cm	3.33 ± 0.13

Figure 2 shows the metal ion D values as a function of the mTDDGA concentration. Distribution ratios of the actinides and lanthanides increase as the DGA concentration is increased, with an almost linear appearance for the log – log plotted data.

The calculated slopes for the different metal ions are reported in Table 1. The values for the slope for Pu deviates, which could be caused by changes in the oxidation states. For the lanthanides (Figure SI- 3), slopes seem to slightly increase with their mass. The slopes of the linear fitting of the logarithm of the distribution ratio as a function of the logarithm of the ligand concentration indicate a 3:1 stoichiometry for actinides and lanthanides. In Table 1, these values are shown for the actinides and a selection of five lanthanides throughout the series. This is in line with previous results from Me$_2$TODGA. More accurate determination of the stoichiometry could be conducted with time resolved laser fluorescence and EXAFS spectroscopy.[24,25]

Batch extraction with different diastereomers of mTDDGA

In a first set of experiments 0.1 mol L^{-1} of each diastereomer of mTDDGA was tested in Exxsol D80, as that diluent was used in the previous EURO-GANEX process.[18] A concentration of 0.1 mol L^{-1} of each mTDDGA was chosen as the available amount of the pure diastereomers was low, and to be able to directly compare the results to the results of the extraction of Me$_2$TODGA
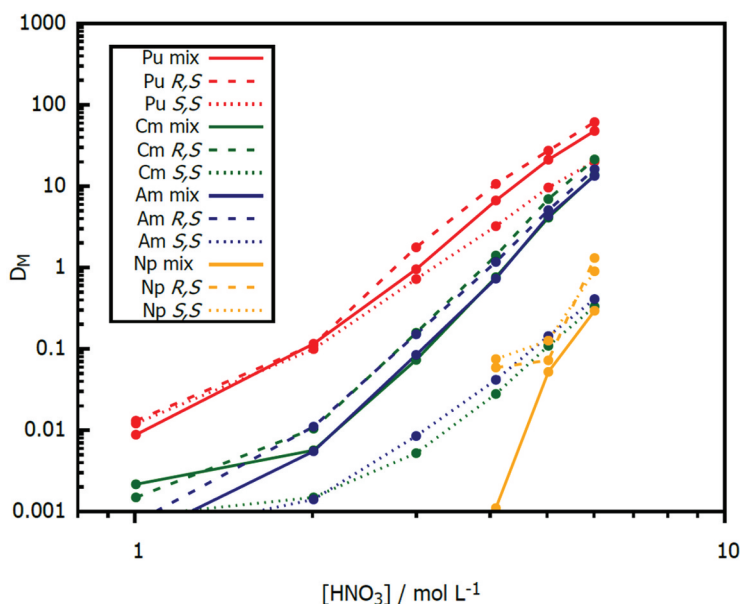

Figure 3. Distribution ratios of [237]Np, [239]Pu, [244]Cm and [241]Am as a function of the nitric acid concentration. Org.: 0.1 mol L^{-1} mTDDGA (different diastereomers) in Exxsol D80. Aq.: 1-6 mol L^{-1} HNO$_3$ containing trace amounts of nonradioactive metals (10^5 mol L^{-1} each) and spiked with radioactive tracers. 22°C, 30 min shaking time.

diastereomers.[25] As known from the scoping study published by Malmbeck et al.[20] we expected significant extraction only at higher nitric acid concentrations. Therefore, we used aqueous phases with nitric acid concentrations between 1-6 mol L^{-1} HNO_3 containing trace amounts of nonradioactive metals (10^{-5} mol L^{-1} each) and spiked with radioactive tracers. The phases were contacted for 30 minutes, which was shown to be sufficient to attain equilibrium. Figure 3 shows the distribution ratios of Np, Pu, and Am as a function of the nitric acid concentration for the (R,S) and (S,S) isomers, and the 3.5:1 ((R,S):(S,S)) mixture of isomers. For Am, a clear difference in the extraction is observed, with the (R,S) isomer extracting the best. The same trend was observed with Time-Resolved Laser-induced Fluorescence Spectroscopy.[56] The (S,S) isomer extracts significantly less and for the mixture distribution ratios in between were observed. Pu extraction was affected less by the orientation of backbone methyl groups, as the difference in extraction between the different diastereomers was rather small. However, the trend (R,S) > mixture > (S,S) isomers was also reproduced by Pu extraction. The Np extraction on the other hand, shows an inconsistent trend. Distribution ratios were quite low, and Np is only extracted significantly at the highest HNO_3 concentrations. Changing oxidation states during extraction might cause higher differences in the extraction than the orientation of the methyl groups and the kinetics might be different for the different experimental series. Therefore, the Np extraction must be further investigated in detail, which was not the scope of the present study.

Figure 3 also shows the distribution ratios of Am and Cm as a function of the nitric acid concentration. Here, the same principal trend is observed, with the (R,S) isomer extracting the best, the (S,S) isomer extracting significantly less and intermediate distribution ratios for the mixture. Interestingly, an inversion of selectivity is observed, similar to the phenomenon that had been observed with the different diastereomers of Me_2 TODGA.[25] The (R,S) isomer and the mixture show a preference for Cm over Am extraction, while the (S,S) isomer shows the opposite selectivity. In Figure SI- 3 in the supporting information, the same data is visualized using a linear scale which gives a clearer view on the absolute differences of the extraction by the (R,S) isomer.

Figure 4 shows an overview of distribution ratios of the metal ions for different diastereomers of mTDDGA and nitric acid concentrations. In these experiments, the important fission products (Sr, Y, Zr, Mo, Tc, Ru, and Pd) and Fe as a corrosion product were also included. Most metal ions show the same trends in nitric acid concentration (increasing distribution ratios with increasing nitric acid concentration) and order of diastereomers ((R,S) > mixture > (S,S)). The lanthanide extraction pattern shows a maximum for the extraction of Er, which is comparable to Me_2 TODGA. This deviates from the extraction behavior of TODGA, which
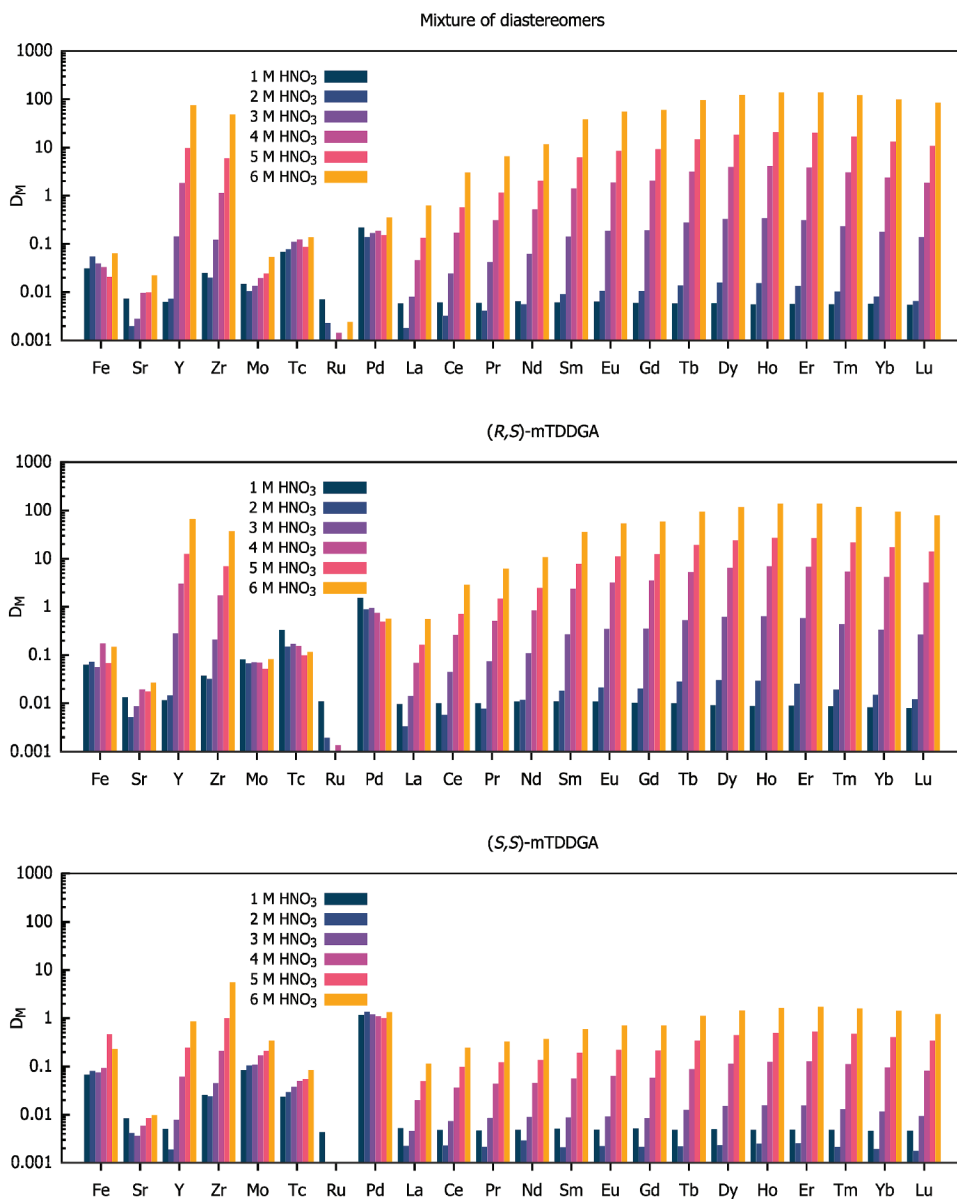
Figure 4. Distribution ratios of all metal ions for different diastereomers of mTDDGA and nitric acid concentrations. Org.: 0.1 mol L^{-1} mTDDGA (different diastereomers) in Exxsol D80. Aq.: 1-6 mol L^{-1} HNO$_3$ containing trace amounts of nonradioactive metals (10^{-5} mol L^{-1}each) and spiked with radioactive tracers. 22°C, 30 min shaking time.

was assigned to sterical effects of the introduced methyl groups.[25] For Ru and Sr, distribution ratios were low under all conditions. Tc is generally weakly extracted but does not follow a clear trend in nitric acid concentration, which could be explained by its extraction as pertechnetate anion. However, it follows the order of diastereomers ((*R,S*)> mixture > (*S,S*)).

The extraction of Fe, Pd, and Mo does not follow the trends. Their distribution ratios are nearly independent of the HNO_3 concentration, and they follow a different order of diastereomers: $(S,S) > (R,S) >$ mixture. Even though it could be possible that the (S,S) isomer extracts these metal ions better, the order of diastereomers is not logical, as the mixture of diastereomers should show an intermediate behavior in any case. Therefore, the Fe, Pd, and Mo extraction is currently not understood and further experiments are needed to understand their behavior.

Solvent extraction with irradiated mTDDGA solvent

From the previously reported experiments, it is clear that one diastereomer is a much better extractant for actinides and lanthanides than the other. Therefore, only the (R,S) diastereomer would be used in practice in a solvent extraction process to keep the solvent extraction system as simple as possible. For further evaluation of the performance towards solvent extraction after gamma irradiation, solutions of the extracting diastereomer (R,S) were irradiated in a ^{60}Co irradiation facility. After centrifugation and phase separation, batch solvent extraction and Pu loading experiments were conducted.

In Figure 5, distribution ratios of Am, Pu, Cm, Eu and Np are shown as a function of absorbed dose, as well as a selection of fission products and lanthanides. The distribution ratios slightly increase during the first 100 kGy of irradiation and then slightly decrease up to 445 kGy. Most remarkable is that the irradiated solvent extracts neptunium significantly better than the fresh solvent, probably due to oxidation of the initial Np(V) by oxidative radicals formed during radiolysis. Similar behavior was observed previously and during the EURO-GANEX development.[16,18,54,57–59]
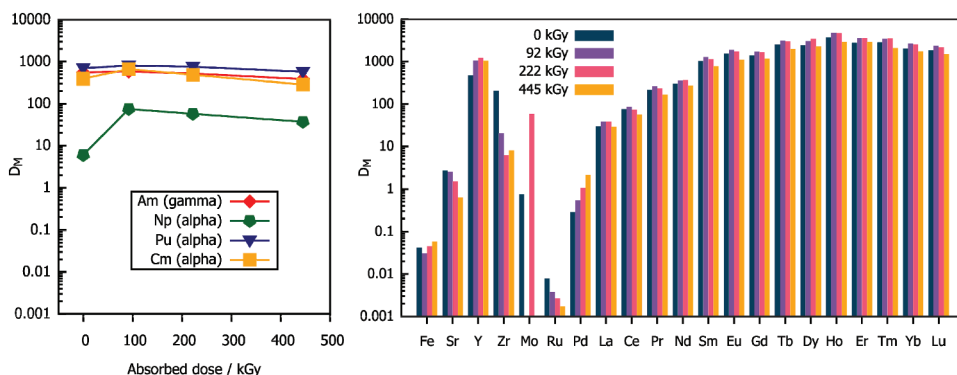

Figure 5. Extraction of Am, Pu, Cm and Np as a function of the absorbed dose for the organic phase irradiated in contact with 5 mol L^{-1} HNO_3. Initial org. 0.5 mol L^{-1} (R,S) mTDDGA in Exxsol D80, aq phase: 5 mol L^{-1} HNO_3, [Ln], [Y] = 1×10⁻⁵ mol L^{-1}, 2.78 kBq ^{152}Eu, 2.81 kBq ^{241}Am, 1.51 kBq ^{244}Cm, 3.23 kBq ^{239}Pu; 0.74 kBq ^{237}Np, 25°C, 60 min, 2500 rpm.

Figure 5 also shows the distribution ratios of the nonradioactive elements as a function of absorbed dose. The lanthanide distribution ratios slightly increase during the first 100 kGy of irradiation and then slightly decrease. This is an indication that formed degradation compounds have extracting properties as well. Degradation compounds with strong complexing properties have been observed for *N*-donor ligands, such as 2,9-bis(5,5,8,8-tetramethyl-5,6,7,8-tetra-hydro-1,2,4-benzotriazin-3-yl)-1,10-phenanthroline (CyMe$_4$BTPhen).[29,60,61] The Ln extraction pattern does not change significantly with an increasing absorbed gamma dose. Here, holmium is the lanthanide with the highest distribution ratio, independent of the absorbed dose, but as the *D* values were high due to the high ligand concentration and high acidity, the difference to the observed maximum for Er above is not considered meaningful.

The extraction of Zr and Ru seems to decrease with increasing dose. Masking of Zr and Pd should be possible with CDTA, as has been shown for TODGA based solvents, and should be tested in the future for mTDDGA.[19] It should be noted that the mass balances for Zr, Mo and Pd during ICP-MS measurements were not consistent. There might be the formation of a small amount of precipitate which cannot be observed visually due to the low metal concentrations. The possible formation of precipitates is an important issue in process development and will be addressed in the future studies with higher metal concentrations.

(*R,S*)-mTDDGA solvents irradiated up to 445 kGy were contacted with a Pu(IV) solution containing 36.2 g L^{-1} Pu(IV), to study possible loading capacity issues. In the supporting information, Figure SI- 4 shows a photograph of the vials after shaking and centrifugation. It shows no visible precipitation and clean organic and aqueous phases. Due to the colored organic and colorless aqueous phase, nearly quantitative Pu extraction was expected. Table 2 shows the organic phase Pu concentrations as a function of the absorbed dose. The values in the column with [Pu]$_{org1}$were determined by measurement of two AHA back-extractions. The values in the third column are the result of subtracting the Pu concentration in the aqueous phase from the Pu concentration in the feed solution. Due to high dilution factors necessary for ICP-MS measurements there is added uncertainty on the data

Table 2. Pu concentration in the irradiated solvents of 0.5 mol L^{-1} (*R,S*)-mTDDGA in Exxsol D80, determined by measurements after back extraction ([Pu]$_{org1}$) with 4 mol L^{-1}AHA in 0.3 mol L^{-1} HNO$_3$, and by calculation based on measurements of the aqueous phase ([Pu]$_{org2}$). There is no data available (N/A) for [Pu]$_{org2}$ for the two intermediate absorbed doses.

Absorbed dose (kGy)	[Pu]$_{org1}$(g L^{-1})	[Pu]$_{org2}$(g L^{-1})	Distribution ratio
0	33.6 ± 3	36.2 ± 4	≥1000
92	28.8 ± 3	N/A	
222	32.5 ± 3	N/A	
445	36.2 ± 4	36.2 ± 4	≥1000

in Table 2. However, even after receiving 445 kGy absorbed dose, the (R,S)-mTDDGA solvent shows the initial high Pu loading capacity. This is an important result for further process development, as the formation of precipitates or a large reduction in Pu loading capacity would have been problematic.

Quantification of degradation compounds in irradiated mTDDGA solvent

In previous work, many degradation compounds of mTDDGA were identified in gamma irradiated solutions using high resolution HPLC-MS.[33] A selection of these degradation compounds was synthesized and used for quantification in irradiated mTDDGA solutions. The chemical structures of these synthesized degradation products are shown in Figure 6.

In Figure 7, quantification of the different main degradation compounds is visualized for increasing absorbed doses. The initial concentration of mTDDGA (mixed diastereomers) was $0.05 \, \text{mol} \, L^{-1}$ in n-dodecane. n-Dodecane was used as the diluent in these experiments to simplify the HPLC-MS analysis, as Exxsol-D80 comprises a mixture of different linear and branched aliphatic hydrocarbons which would make the radiation chemistry more complicated. The samples irradiated in contact with $2.5 \, \text{mol} \, L^{-1}$ nitric acid contained a small amount of precipitate. Hence, centrifugation before taking samples for HPLC-MS was essential.

Compound DC III, C_{ether}-O_{ether} bond breaking product, was the most abundant radiolysis product, independent of the chemical conditions during irradiation. It reached the highest concentrations after 250–500 kGy absorbed dose. After that, the concentration in the organic phase decreased again. This means that the production rate by degradation of the initial mTDDGA becomes lower than the degradation rate of the DC itself. Other contributions
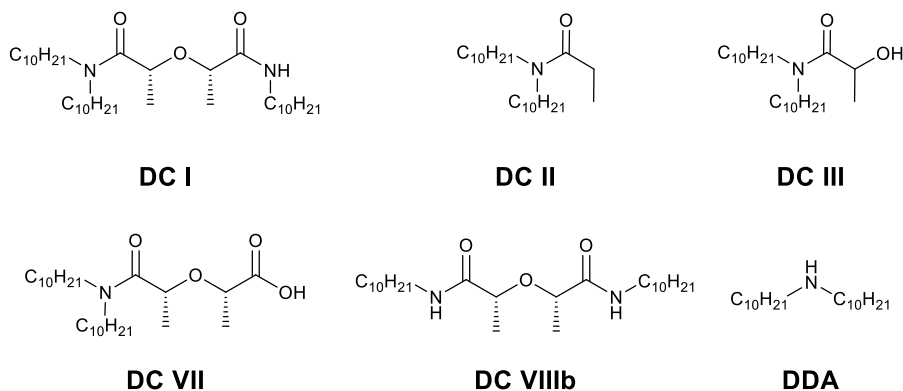

Figure 6. Degradation compounds of (R,S)-mTDDGA used for quantification.

to DC III production could be the radiolysis of DC VII, DC I or an addition reaction of DC II with $^{\bullet}$OH radicals.

In samples irradiated without contact to an aqueous phase, the concentration of the amide DC II increased with increasing absorbed doses. On the other hand, it was not detected in quantifiable concentrations in the samples irradiated in contact with nitric acid (<0.5 mmol L^{-1}). Possibly, in the presence of the aqueous phase, the formation of DC III is more probable because of the radiolytic formation of $\bullet$OH radicals from water. This behavior is comparable to the radiolysis of TODGA. However, in the case of TODGA the most important degradation compound became the acetamide (the equivalent of DC II) in absence of nitric acid, which is not the case for mTDDGA.[46] In the same study, pre-equilibration with nitric acid also strongly promoted the production of the TODGA equivalent of DC III. Hubscher-Bruder et al. also observed for Me-TODGA that the main degradation products in nitric acid pre-equilibrated samples were these DC III equivalents, for which two options exist due to the asymmetrical nature of this single methylated ligand.[39]

The single de-alkylated radiolysis product of mTDDGA (DC I) is more abundant in the organic phases which are irradiated in contact with the aqueous nitric acid phases. The double de-alkylated degradation product (DC VIIIb) is the result of the radiolysis of DC I. It is only present in low concentrations and mainly in the organic phases which were contacted with nitric acid. These products both still contain the diglycolamide structure, and therefore could be capable of forming complexes with metal ions. The extraction behavior of DC I is further studied in this paper. The extraction behavior of DC VIIIb was not studied, because the solubility in *n*-dodecane was too low. Therefore, radiolytic production of this compound during operation of the solvent extraction process could be expected to contribute to precipitation.
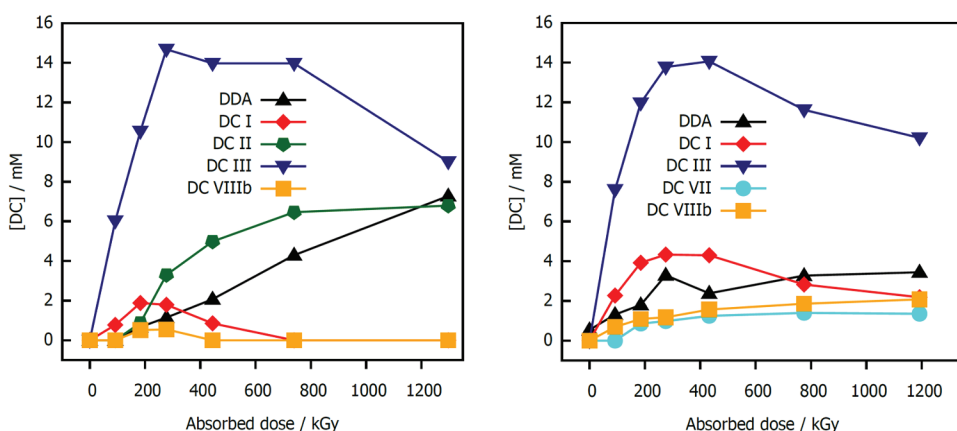

Figure 7. Quantification of DCs in irradiated 0.05 mol L^{-1} mTDDGA in *n*-dodecane, irradiated without contact to an aqueous phase (top) and irradiated in contact with 2.5 mol L^{-1} HNO$_3$ (bottom).

The acidic degradation compound DC VII was only present in the samples irradiated in contact with nitric acid in quantifiable amounts. This is the result of de-amination of mTDDGA followed by end-capping with $^{\bullet}$OH, which is an explanation for its presence in samples irradiated in contact with nitric acid.

In the samples irradiated without contact to an aqueous phase, the concentration of di-n-decylamine (DDA) increased with increasing absorbed dose. These samples did not contain any precipitates. DDA is formed by de-amination from mTDDGA, but also from secondary de-amination reaction of the DCs. In the samples irradiated in contact with nitric acid, DDA was protonated and precipitated, as it is not soluble in n-dodecane nor in the nitric acid solution. In the samples irradiated in contact with nitric acid, the DDA concentration stagnates just under 4 mmol L^{-1}. The excess of the formed DDA precipitates at the interphase which was proven by HPLC-MS analysis of the separated precipitate. Analysis of the precipitate, which was separated by filtration of an irradiated sample (454 kGy) of 0.05 mol L^{-1} mTDDGA in n-dodecane contacted with 2.5 mol L^{-1} HNO$_3$, showed only the presence of a low concentration of DC I (0.6 mmol L^{-1}) and mainly the presence of 2.7 mmol L^{-1} of DDA. The sample (irradiated up to 445 kGy) using the other sample preparation method (methanol wash) contained 0.2 mmol L^{-1} of mTDDGA and 11.7 mmol L^{-1} DDA.

Batch solvent extraction with DC I

Batch solvent extractions were only performed with DC I, DC II and DC III due to the limited solubility of the other DCs in an aliphatic diluent. The single de-alkylation degradation compound DC I still has the original diglycolamide backbone as the core of its structure. Throughout the experimental series with increasing nitric acid concentrations ≥4 mol L^{-1} HNO$_3$, increasing precipitate formation was observed. DC I contains a secondary amide function, which is probably protonated by higher HNO$_3$concentrations, and the protonated form is less soluble in the solvent. This could be a reason for the observation of a drop in the distribution ratios for all Ln and An in Figure 8, except for Pu and Np (for which the increasing nitric acid concentration probably also affects their oxidation state). For the fission product Pd, the mass balance was extremely low (<10%), which strongly indicates the formation of precipitate. Pu is best extracted element, with distribution ratios of about one order of magnitude higher than for the other actinides.

Extraction increased as the concentration of DC I in the organic phase increased for the first part of the curve as expected, as shown for the radioactive elements as for the nonradioactive elements in Figure 9. However, at concentrations higher than 0.1 mol L^{-1} DC I, there is a clear kink in the curves. This is also the point at which precipitation was visually observed at the interphases during the experiments. This means that it is, strictly speaking, not possible to determine a distribution ratio for the two phases, since there are three phases
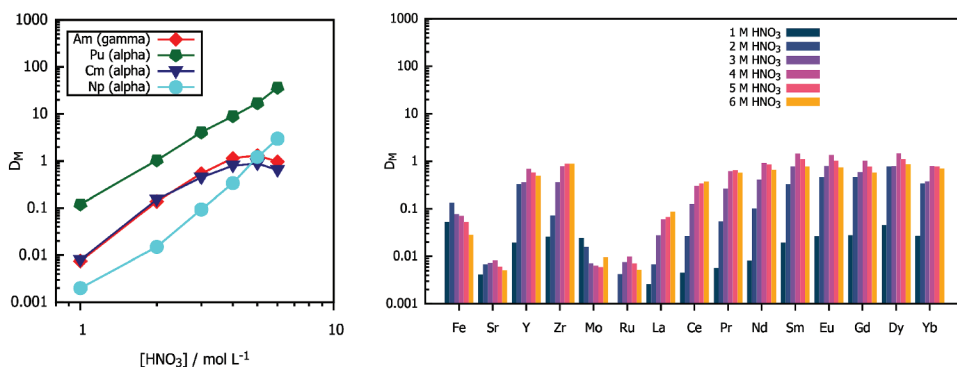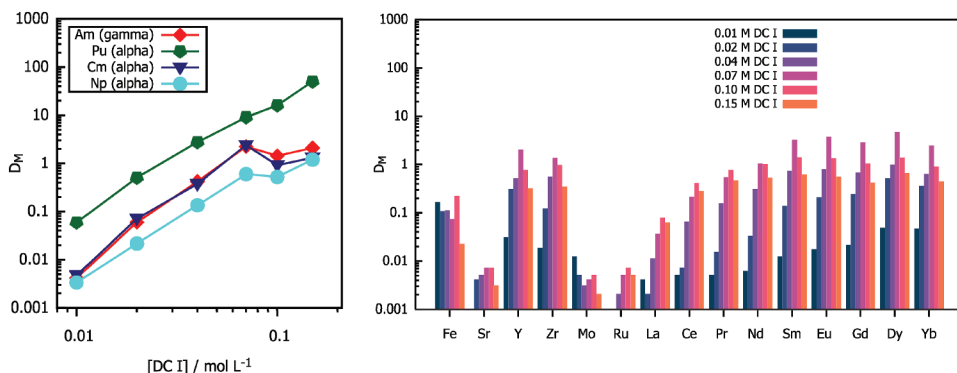
Figure 8. Distribution ratios of radiotracer elements by α and γ spectrometry (left) and ICP-MS for nonradioactive metal ions (right) as a function of the HNO_3 concentration: [DC I] = 0.1 mol L^{-1}, 1 h, [M] = 10^{-5} mol L^{-1}, 25°C, ±1 kBq of ^{152}Eu, ^{237}Np, ^{239}Pu, ^{241}Am, ^{244}Cm.

Figure 9. Distribution ratios of radiotracer elements by α and γ spectrometry (left) and ICP-MS for nonradioactive metal ions (right) as a function of the DC I concentration: [HNO_3] = 5 mol L^{-1}, 1 h, [M] = 10^{-5} mol L^{-1}, 25°C, ±1 kBq of ^{152}Eu, ^{237}Np, ^{239}Pu, ^{241}Am, ^{244}Cm.

from this point on. Interestingly, the only element which is mostly unaffected is Pu. Slope analyses for only the first four data points at the lowest ligand concentrations indicate towards 3:1 complexes with trivalent actinides (Am slope of 3.26 ± 0.16, R^2 = 0.995 and Cm slope of 3.24 ± 0.15, R^2 = 0.996).

These findings are generally in agreement with previous work on TODGA and methylated TODGA derivatives. Galán et al. reported only significant distribution ratios (>0.1) for the TODGA equivalents of DC VII (which did not dissolve sufficiently), DC III and DC I. Solvent extraction with degradation compounds of MeTODGA, more specifically 2-hydroxyoctylamides (similar to DC III, but shorter alkyl chains), showed extraction of metal ions.[39] However, the authors did not study the extraction of Pu, which was shown here to be the best extracted actinide.

Batch solvent extraction with DC II

In Figure 10, the distribution ratios for Pu and Np are expressed as a function of the nitric acid concentration. For the other radiotracers (Am, Cm and Eu), D ratios were below 0.001 or below the detection limit of the α/γ spectrometer. The distribution ratios for Pu and Np remained far below 1.

In Figure 11, distribution ratios for the radiotracer elements are shown as a function of increasing ligand concentration. At high concentrations of this DC II, there is some extraction of Pu observed. However, the distribution ratios are still very low, as expected from an initial screening experiment. The slopes of the $\log([D])/\log([L])$ plots are 2.3 ± 0.04 ($R^2 = 0.999$) and 2.4 ± 0.1 ($R^2 = 0.988$) for Pu and Np, respectively, indicating mainly 2:1 complexation. This is similar to other extracting amides.[48]

Batch solvent extraction with DC III

Distribution ratios of the radioactive tracers and other metal ions are shown as a function of the nitric acid concentration in Figure 12. DC III extracts Pu with a high distribution ratio at high acidities. Distribution ratios of over 100 were measured at 5 mol L^{-1} HNO_3. The other An and Ln reached a maximum D value of about 1. Zr is extracted rather well, with distribution ratios up to about 100. Possibly the use of a masking agent such as CDTA will reduce this.[19] Low mass balances of <50% make it difficult to evaluate Mo and Pd extraction. Since DC III is the most abundant DC of mTDDGA, it is possibly responsible
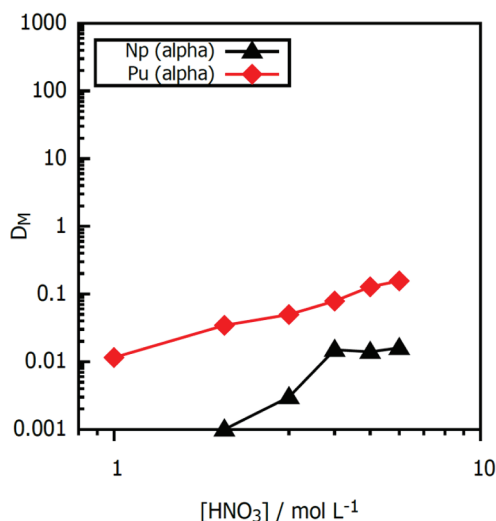
Figure 10. Np and Pu distribution ratios (alpha spectrometry) as a function of the initial nitric acid concentration of the aqueous phase: DC II = 0.1 mol L^{-1}, 1 h, [M] = 10^{-5} mol L^{-1}, 25°C, 1 kBq of ^{152}Eu, ^{237}Np, ^{239}Pu, ^{241}Am, ^{244}Cm. for Am, Cm and Eu, D ratios were below 0.001 or below the detection limit of the α/γ spectrometer.
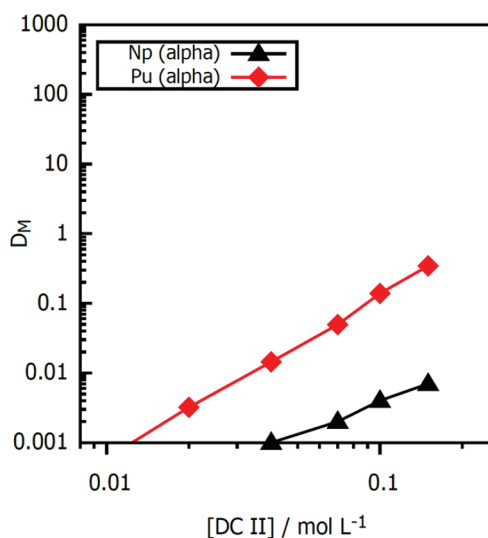
Figure 11. Distribution ratios of radiotracer elements by α spectrometry as a function of the DC II concentration: $[HNO_3] = 5$ mol L^{-1}, 1 h, $[M] = 10^{-5}$ mol L^{-1}, 25°C, 1 kBq of ^{152}Eu, ^{237}Np, ^{239}Pu, ^{241}Am, ^{244}Cm. for Am, Cm and Eu, D ratios were below 0.001 or below the detection limit of the α/γ spectrometer.
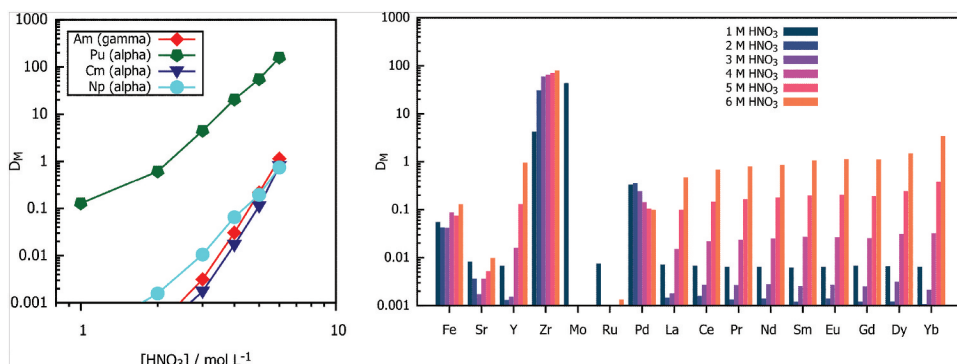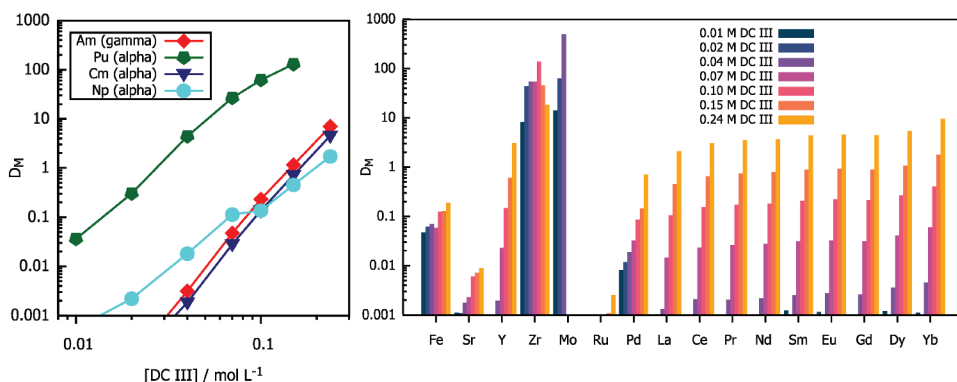

Figure 12. Distribution ratios of radiotracer elements by α and γ spectrometry (left) and ICP-MS for nonradioactive metal ions (right) as a function of the initial nitric acid concentration of the aqueous phase: DC III = 0.1 mol L^{-1}, 1 h, $[M] = 10^{-5}$ mol L^{-1}, 25°C, 1 kBq of ^{152}Eu, ^{237}Np, ^{239}Pu, ^{241}Am, ^{244}Cm.

for the efficient extraction of Pu, even after the mTDDGA solvent received high gamma doses.

In Figure 13, the concentration of DC III was varied at 5 mol L^{-1} HNO_3. The distribution ratios of Mo quickly increased with increasing ligand concentration, but then suddenly dropped below 0.001 at ligand concentrations ≥0.07 mol L^{-1}. Mass balances dropped significantly as well

Figure 13. Distribution ratios of radiotracer elements by α and γ spectrometry (left) and ICP-MS for nonradioactive metal (right) ions as a function of the DC III concentration: $[HNO_3] = 5$ mol L^{-1}, 1 h, $[M] = 10^{-5}$ mol L^{-1}, 25°C, ±1 kBq of ^{152}Eu, ^{237}Np, ^{239}Pu, ^{241}Am, ^{244}Cm.

at ligand concentrations ≥0.07 mol L^{-1} (below 50%), strongly indicating the formation of a precipitate. Palladium is also extracted, but only reaching a distribution ratio of 1 at the highest DC concentration. In general, lanthanide extraction increases as the DC concentration increases, but only reaching above 1 for the highest DC concentration(s). Heavier lanthanides seem to be more efficiently extracted, in contrast to the mTDDGA itself which reaches a maximum at Ho.

Conclusions

Extraction by mTDDGA is fast under the tested batch extraction conditions for the actinides and most of the lanthanides. Complexation behavior is as expected and typical for diglycolamides, forming mainly 3:1 complexes with trivalent actinides and lanthanides. The (R,S) diastereomer, the one with the backbone methyl groups oriented in the same direction, exhibits at least one order of magnitude higher distribution ratios than the (S,S) diastereomer. Using only the (R,S) diastereomer is therefore preferred to avoid additional complexity of solvent clean-up and increased viscosity, although it does require selective synthesis or diastereomeric separation. (R,S)-mTDDGA was found to be stable against gamma-irradiation with slightly increasing actinides and lanthanide distribution ratios up to ca. 100 kGy. This is an indication that certain degradation compounds are good extractants themselves. Further irradiation of the mTDDGA solvent caused a slight decrease of the distribution ratios, although remaining well over 100 for all Ln/An (except for Np). The irradiated solvent was shown to be capable of being loaded with at least 36 g L^{-1} Pu after irradiation up to 445 kGy, by far exceeding the requirement of 10 g L^{-1} initially defined for the

EURO-GANEX process.[18] The most abundant degradation compound of mTDDGA, 2-hydroxydi-*n*-decylamide (DC III), extracts mainly plutonium, with distribution ratios well over 100 for higher HNO_3 concentrations. Extraction of other actinides and the lanthanides was lower by two order of magnitudes. The extraction efficiency of this degradation compound of mTDDGA is likely responsible for its capability to sustain the high Pu loading also at elevated irradiation doses. The amide, DCII, only showed very limited extraction of plutonium. The degradation compound with an intact DGA backbone (DC I) extracts actinides and lanthanides as expected. However, at higher nitric acid concentrations and higher ligand concentrations it forms precipitates. These results are promising towards the further development of a new EURO-GANEX process using a mTDDGA solvent.

Disclosure statement

No potential conflict of interest was reported by the author(s).

ORCID

Bart Verlinden http://orcid.org/0000-0001-6694-3130
Andreas Wilden http://orcid.org/0000-0001-5681-3009
Karen Van Hecke http://orcid.org/0000-0002-7100-192X
Richard J. M. Egberink http://orcid.org/0000-0002-2505-9960
Jurriaan Huskens http://orcid.org/0000-0002-4596-9179
Willem Verboom http://orcid.org/0000-0002-6863-8655
Michelle Hupert http://orcid.org/0000-0002-1179-573X
Andreas Geist http://orcid.org/0000-0003-1436-8247
Marc Verwerft http://orcid.org/0000-0002-2385-6093
Giuseppe Modolo http://orcid.org/0000-0001-6490-5595
Koen Binnemans http://orcid.org/0000-0003-4768-3606
Thomas Cardinaels http://orcid.org/0000-0002-2695-1002

References

[1] Taylor, R. *Reprocessing and Recycling of Spent Nuclear Fuel*; Taylor, R., Ed.; Woodhead Publishing: Oxford, 2015.

[2] Popescu, L. Nuclear-Physics Applications of MYRRHA. *EPJ Web Conf.* 2014, *66*, 10011. DOI: 10.1051/epjconf/20146610011.

[3] Oigawa, H.; Tsujimoto, K.; Nishihara, K.; Sugawara, T.; Kurata, Y.; Takei, H.; Saito, S.; Sasa, T.; Obayashi, H. Role of ADS in the Back-End of the Fuel Cycle Strategies and Associated Design Activities: The Case of Japan. *J. Nucl. Mater.* 2011, *415*(3), 229–236. DOI: 10.1016/j.jnucmat.2011.04.032.

[4] Serp, J.; Poinssot, C.; Bourg, S. Assessment of the Anticipated Environmental Footprint of Future Nuclear Energy Systems. Evidence of the Beneficial Effect of Extensive Recycling. *Energies*. 2017, *10*(9), 9. DOI: 10.3390/en10091445.

[5] Poinssot, C.; Bourg, S.; Ouvrier, N.; Combernoux, N.; Rostaing, C.; Vargas-Gonzalez, M.; Bruno, J. Assessment of the Environmental Footprint of Nuclear Energy Systems. Comparison between Closed and Open Fuel Cycles. *Energy* 2014, *69*, 199–211. DOI: 10.1016/j.energy.2014.02.069.

[6] Poinssot, C.; Bourg, S., and Boullis, B. Improving the Nuclear Energy Sustainability by Decreasing Its Environmental Footprint. Guidelines from Life Cycle Assessment Simulations. *Prog. Nucl. Energy* 2016, *92*, 234–241. DOI: 10.1016/j.pnucene.2015.10.012.

[7] Goff, K. M.; Fredrickson, G. L., and Vaden, D. E. Safeguards Technology for Radioactive Materials Processing and Nuclear Fuel Reprocessing Facilities. In *Advanced Separation Techniques for Nuclear Fuel Reprocessing and Radioactive Waste Treatment*; Nash , and K. L., and Lumetta, G. J., Eds.; Woodhead Publishing: Oxford, UK; Philadelphia, PA, 2011; pp 120–137.

[8] Adnet, J.-M.; Miguirditchian, M.; Hill, C.; Heres, X.; Lecomte, M.; Masson, M.; Brossard, P.; Baron, P. Development of New Hydrometallurgical Processes for Actinide Recovery: GANEX Concept. Proceedings of GLOBAL, Tsukuba, Japan, Oct 9–13, 2005.

[9] Miguirditchian, M.; Sorel, C.; Camès, B.; Bisel, I.; Baron, P.; Espinoux, D.; Calor, J.-N.; Viallesoubranne, C.; Lorrain, B., and Masson, M. HA Demonstration in the Atalante Facility of the Ganex 1st Cycle for the Selective Extraction of Uranium from HLW. Proceedings of GLOBAL, Paris, France, Sep 6–11, 2009; pp. 1032–1035.

[10] Miguirditchian, M.; Chareyre, L.; Sorel, C.; Bisel, I.; Baron, P., and Masson, M. Development of the GANEX Process for the Reprocessing of Gen IV Spent Nuclear Fuels. ATALANTE meeting, Montpellier, France, 2008.

[11] Miguirditchian, M.; Roussel, H.; Chareyre, L.; Baron, P.; Espinoux, D.; Calor, J.-N.; Viallesoubranne, C.; Lorrain, B., and Masson, M. HA Demonstration in the Atalante Facility of the GANEX 2ndCycle for the Grouped TRU Extraction. Proceedings of GLOBAL, Paris, France, Sep 6–11, 2009; pp. 1036–1040.

[12] Bourg, S.; Hill, C.; Caravaca, C.; Rhodes, C.; Ekberg, C.; Taylor, R.; Geist, A.; Modolo, G.; Cassayre, L.; Malmbeck, R., et al. Acsept—partitioning Technologies and Actinide Science: Towards Pilot Facilities in Europe. *Nucl. Eng. Des.* 2011, *241*(9), 3427–3435. DOI: 10.1016/j.nucengdes.2011.03.011.

[13] Bourg, S.; Poinssot, C.; Geist, A.; Cassayre, L.; Rhodes, C., and Ekberg, C. Advanced Reprocessing Developments in Europe Status on European Projects ACSEPT and ACTINET-I3. *Procedia Chem.* 2012, *7*, 166–171. DOI: 10.1016/j.proche.2012.10.028.

[14] Joly, P., and Boo, E. SACCSESS Roadmap: Actinide Separation Processes. In *Euratom Research and Training Programme on Nuclear Energy Within the Seventh Framework Programme*; Paris, France, 2015.

[15] Geist, A.; Taylor, R.; Ekberg, C.; Guilbaud, P.; Modolo, G., and Bourg, S. The SACSESS Hydrometallurgy Domain — an Overview. *Procedia Chem.* 2016, *21*, 218–222. DOI: 10.1016/j.proche.2016.10.031.

[16] Carrott, M.; Bell, K.; Brown, J.; Geist, A.; Gregson, C.; Hères, X.; Maher, C.; Malmbeck, R.; Mason, C., and Modolo, G., et al. Development of a New Flowsheet for Co-Separating the Transuranic Actinides: The "EURO-GANEX" Process. *Solvent Extr. Ion Exch.* 2014, *32*(5), 447–467. DOI: 10.1080/07366299.2014.896580.

[17] Bell, K.; Carpentier, C.; Carrott, M.; Geist, A.; Gregson, C.; Hérès, X.; Magnusson, D.; Malmbeck, R.; McLachlan, F., and Modolo, G., et al. Progress Towards the Development of a New GANEX Process. *Procedia Chem.* 2012, *7*, 392–397. DOI: 10.1016/j.proche.2012.10.061.

[18] Malmbeck, R.; Magnusson, D.; Bourg, S.; Carrott, M.; Geist, A.; Hérès, X.; Miguirditchian, M.; Modolo, G.; Müllich, U., and Sorel, C., et al. Homogenous Recycling of Transuranium Elements from Irradiated Fast Reactor Fuel by the EURO-GANEX Solvent Extraction Process. *Radiochim. Acta* 2019, *107*(9–11), 917–929. DOI: 10.1515/ract-2018-3089.

[19] Sypula, M.; Wilden, A.; Schreinemachers, C.; Malmbeck, R.; Geist, A.; Taylor, R., and Modolo, G. Use of Polyaminocarboxylic Acids as Hydrophilic Masking Agents for Fission Products in Actinide Partitioning Processes. *Solvent Extr. Ion Exch.* 2012, *30* (7), 748–764. DOI: 10.1080/07366299.2012.700591.

[20] Malmbeck, R.; Magnusson, D., and Geist, A. Modified Diglycolamides for Grouped Actinide Separation. *J. Radioanal. Nucl. Chem.* 2017, *314*(3), 2531–2538. DOI: 10.1007/s10967-017-5614-2.

[21] Brown, J.; McLachlan, F.; Sarsfield, M.; Taylor, R.; Modolo, G., and Wilden, A. Plutonium Loading of Prospective Grouped Actinide Extraction (GANEX) Solvent Systems Based on Diglycolamide Extractants. *Solvent. Extr Ion Exch.* 2012, *30*(2), 127–141. DOI: 10.1080/07366299.2011.609378.

[22] Sasaki, Y.; Sugo, Y.; Suzuki, S., and Kimura, T. A Method for the Determination of Extraction Capacity and Its Application to Alkylderivatives of Diglycolamide-Monoamide/n-Dodecane Media. *Anal Chim. Acta.* 2005, *543*(1–2), 31–37. DOI: 10.1016/j.aca.2005.04.061.

[23] Iqbal, M.; Huskens, J.; Verboom, W.; Sypula, M., and Modolo, G. Synthesis and Am/eu Extraction of Novel TODGA Derivatives. *Supramol. Chem.* 2010, *22*(11–12), 827–837. DOI: 10.1080/10610278.2010.506553.

[24] Wilden, A.; Modolo, G.; Lange, S.; Sadowski, F.; Beele, B. B.; Skerencak-Frech, A.; Panak, P. J.; Iqbal, M.; Verboom, W., and Geist, A., et al. Modified Diglycolamides for the An(iii) + Ln(iii) Co-Separation: Evaluation by Solvent Extraction and Time-Resolved Laser Fluorescence Spectroscopy. *Solvent Extr. Ion Exch.* 2014, *32*(2), 119–137. DOI: 10.1080/07366299.2013.833791.

[25] Wilden, A.; Kowalski, P. M.; Klass, L.; Kraus, B.; Kreft, F.; Modolo, G.; Li, Y.; Rothe, J.; Dardenne, K., and Geist, A., et al. Unprecedented Inversion of Selectivity and Extraordinary Difference in the Complexation of Trivalent *F*-Elements by Diastereomers of a Methylated Diglycolamide. *Chem. Eur. J.* 2019, *25*(21), 5507–5513. DOI: 10.1002/chem.201806161.

[26] Manion, J. P., and Burton, M. Radiolysis of Hydrocarbon Mixtures. *J. Phys. Chem.* 1952, *56*(5), 560–569. DOI: 10.1021/j150497a005.

[27] Wojnárovits, L., and Földiák, G. Structure Effect in Alkane Radiolysis. *Radiat. Res.* 1982, *91*(3), 638–643. DOI: 10.2307/3575898.

[28] Mincher, B. J.; Modolo, G., and Mezyk, S. P. Review Article: The Effects of Radiation Chemistry on Solvent Extraction: 1. Conditions in Acidic Solution and a Review of TBP Radiolysis. *Solvent Extr. Ion Exch.* 2009, *27*(1), 1–25. DOI: 10.1080/07366290802544767.

[29] Zsabka, P.; Van Hecke, K.; Wilden, A.; Modolo, G.; Hupert, M.; Jespers, V.; Voorspoels, S.; Verwerft, M.; Binnemans, K., and Cardinaels, T. Gamma Radiolysis of TODGA and CyMe$_4$BTPhen in the Ionic Liquid Tri-*N*-Octylmethylammonium Nitrate. *Solvent. Extr Ion Exch.* 2020, *38*(2), 212–235. DOI: 10.1080/07366299.2019.1710918.

[30] Mincher, B. J.; Modolo, G., and Mezyk, S. P. Review Article: The Effects of Radiation Chemistry on Solvent Extraction 3: A Review of Actinide and Lanthanide Extraction. *Solvent Extr. Ion Exch.* 2009, *27*(5–6), 579–606. DOI: 10.1080/07366290903114098.

[31] Mincher, B. J.; Modolo, G., and Mezyk, S. P. Review: The Effects of Radiation Chemistry on Solvent Extraction 4: Separation of the Trivalent Actinides and Considerations for Radiation-Resistant Solvent Systems. *Solvent Extr. Ion Exch.* 2010, *28*(4), 415–436. DOI: 10.1080/07366299.2010.485548.

[32] Sugo, Y.; Sasaki, Y., and Tachimori, S. Studies on Hydrolysis and Radiolysis of *N,N,N′,N′*-Tetraoctyl-3-Oxapentane-1,5-Diamide. *Radiochim. Acta* 2002, *90*(3), 161–165. DOI: 10.1524/ract.2002.90.3_2002.161.

[33] Verlinden, B.; Van Hecke, K.; Wilden, A.; Hupert, M.; Modolo, G.; Verwerft, M.; Binnemans, K., and Cardinaels, T. Gamma radiolytic stability of the novel modified diglycolamide 2,2'-oxybis(*N,N*-didecylpropanamide) (mTDDGA) for grouped actinide extraction. *RSC Adv.* 2022, *12*, 12416–12426. DOI: 10.1039/D1RA08761D.

[34] Horne, G. P.; Wilden, A.; Mezyk, S. P.; Twight, L.; Hupert, M.; Stark, A.; Verboom, W.; Mincher, B. J., and Modolo, G. Gamma Radiolysis of Hydrophilic Diglycolamide Ligands in Concentrated Aqueous Nitrate Solution. *Dalton Trans.* 2019, *48*(45), 17005–17013. DOI: 10.1039/c9dt03918j.

[35] Roscioli-Johnson, K. M.; Zarzana, C. A.; Groenewold, G. S.; Mincher, B. J.; Wilden, A.; Schmidt, H.; Modolo, G., and Santiago-Schübel, B. A Study of the γ-Radiolysis of *N,N*-Didodecyl-*N′,N′*-Dioctyldiglycolamide Using UHPLC-ESI-MS Analysis. *Solvent Extr. Ion Exch.* 2016, *34*(5), 439–453. DOI: 10.1080/07366299.2016.1212540.

[36] Wilden, A.; Mincher, B. J.; Mezyk, S. P.; Twight, L.; Rosciolo-Johnson, K. M.; Zarzana, C. A.; Case, M. E.; Hupert, M.; Stark, A., and Modolo, G. Radiolytic and Hydrolytic Degradation of the Hydrophilic Diglycolamides. *Solvent. Extr. Ion Exch.* 2018, *36*(4), 347–359. DOI: 10.1080/07366299.2018.1495384.

[37] Galán, H.; Zarzana, C. A.; Wilden, A.; Nunez, A.; Schmidt, H.; Egberink, R. J. M.; Leoncini, A.; Cobos, J.; Verboom, W., and Modolo, G., et al. Gamma-Radiolytic Stability of New Methylated TODGA Derivatives for Minor Actinide Recycling. *Dalton Trans.* 2015, *44*(41), 18049–18056. DOI: 10.1039/c5dt02484f.

[38] Zarzana, C. A.; Groenewold, G. S.; Mincher, B. J.; Mezyk, S. P.; Wilden, A.; Schmidt, H.; Modolo, G.; Wishart, J. F., and Cook, A. R. A Comparison of the γ-Radiolysis of TODGA and T(EH)DGA Using UHPLC-ESI-MS Analysis. *Solvent Extr. Ion Exch.* 2015, *33*(5), 431–447. DOI: 10.1080/07366299.2015.1012885.

[39] Hubscher-Bruder, V.; Mogilireddy, V.; Michel, S.; Leoncini, A.; Huskens, J.; Verboom, W.; Galán, H.; Núñez, A.; Cobos, J., and Modolo, G., et al. Behaviour of the Extractant Me-TODGA Upon Gamma Irradiation: Quantification of Degradation Compounds and Individual Influences on Complexation and Extraction. *New. J. Chem.* 2017, *41*(22), 13700–13711. DOI: 10.1039/c7nj02136d.

[40] Mincher, B. J., and Curry, R. D. Considerations for Choice of a Kinetic Fig. Of Merit in Process Radiation Chemistry for Waste Treatment. *Appl. Radiat. Isot.* 2000, *52*(2), 189–193. DOI: 10.1016/s0969-8043(99)00161-x.

[41] Mezyk, S. P.; Mincher, B. J.; Dhiman, S. B.; Layne, B., and Wishart, J. F. The Role of Organic Solvent Radical Cations in Separations Ligand Degradation. *J. Radioanal. Nucl. Chem.* 2015, *307*(3), 2445–2449. DOI: 10.1007/s10967-015-4582-7.

[42] Mezyk, S. P.; Horne, G. P.; Mincher, B. J.; Zalupski, P. R.; Cook, A. R., and Wishart, J. F. The Chemistry of Separations Ligand Degradation by Organic Radical Cations. *Procedia Chem.* 2016, *21*, 61–65. DOI: 10.1016/j.proche.2016.10.009.

[43] Horne, G. P.; Gregson, C. R.; Sims, H. E.; Orr, R. M.; Taylor, R. J., and Pimblott, S. M. Plutonium and Americium Alpha Radiolysis of Nitric Acid Solutions. *J. Phys. Chem. B.* 2017, *121*(4), 883–889. DOI: 10.1021/acs.jpcb.6b12061.

[44] Nagaishi, R.; Jiang, P. Y.; Katsumura, Y.; Domae, M., and Ishigure, K. Radiolysis of Concentrated Nitric Acid Solutions. Proceedings of the 6th Japan-China bilateral symposium on radiation chemistry, Tokyo, Japan, 1995.

[45] Le Caër, S. Water Radiolysis: Influence of Oxide Surfaces on H_2 Production Under Ionizing Radiation. *Water* 2011, *3*(1), 235–253. DOI: 10.3390/w3010235.

[46] Galán, H.; Núñez, A.; Espartero, A. G.; Sedano, R.; Durana, A., and de Mendoza, J. Radiolytic Stability of TODGA: Characterization of Degraded Samples Under Different Experimental Conditions. *Procedia Chem.* 2012, *7*, 195–201. DOI: 10.1016/j.proche. 2012.10.033.

[47] John, J., Kalvoda, L., Celbova, L., Fojtikova, J., Koubsky, T., Lutinec, J., Verlinden, B.; Kowalski, P. M.; ; Wilden, A., and Modolo, G. *Molecular modelling of particular degradation mechanism of extracting and complexing agents. GENIORS Deliverable D2.5*; Czech Technical University: Prague, 2020. https://www.geniors.eu/public-library/

[48] Siddall, T. H. Effects of Structure of *N,N*-Disubstituted Amides on Their Extraction of Actinide and Zirconium Nitrates and of Nitric Acid. *J. Phys. Chem.* 1960, *64*(12), 1863–1866. DOI: 10.1021/j100841a014.

[49] Feder, H. M., and Vogel, R. C. *Extraction Process Chemistry of Uranium and Plutonium Complexing Agents More Effective Than TBP*; ANL-4675; Argonne National Laboratory: USA, 1951.

[50] Danesi, P. R. The Meaning of Slope Analysis in Solvent Extraction Chemistry. 1969.

[51] Rydberg, J.; Cox, M.; Musikas, C., and Choppin, G. R. *Solvent Extraction Principles and Practice*, 22nd ed. Marcel Dekker Inc.: New York, 2005; p. 480.

[52] Verlinden, B.; Zsabka, P.; Van Hecke, K.; Verguts, K.; Mihailescu, L.-C.; Modolo, G.; Verwerft, M.; Binnemans, K.; Cardinaels, T. Dosimetry and Methodology of Gamma Irradiation for Degradation Studies on Solvent Extraction Systems. *Radiochim. Acta* 2021, *109*(1), 61–72. DOI: 10.1515/ract-2020-0040.

[53] Fein, M. L., and Filachione, E. M. Ester-Amides of Lactic Acid. *J. Am. Chem. Soc.* 1953, *75*(9), 2099–2101. DOI: 10.1021/ja01105a023.

[54] Carrot, M. J.; Gregson, C. R.; Taylor, R. J. Neptunium Extraction and Stability in the GANEX Solvent: 0.2 M TODGA/0.5 M Dmdohema/kerosene. *Solvent Extr. Ion Exch.* 2013, *31*(5), 463–482. DOI: 10.1080/07366299.2012.735559.

[55] Siddall, T. H., and Dukes, E. K. Kinetics of HNO_2 Catalyzed Oxidation of Neptunium(v) by Aqueous Solutions of Nitric Acid. *J. Am. Chem. Soc.* 1959, *81*(4), 790–794. DOI: 10. 1021/ja01513a007.

[56] Weßling, P.; Trumm, M.; Sittel, T.; Geist, A.; Panak, P. J. Spectroscopic Investigation of the Different Complexation and Extraction Properties of Diastereomeric Diglycolamide Ligands. *Radiochim. Acta* 2022, *110*(5), 291–300. DOI: 10.1515/ract-2021-1134.

[57] Precek, M.; Paulenova, A., and Mincher, B. J. Reduction of Np(vi) in Irradiated Solutions of Nitric Acid. *Procedia Chem.* 2012, *7*, 51–58. DOI: 10.1016/j.proche.2012.10.010.

[58] Horne, G. P.; Grimes, T. S.; Mincher, B. J.; Mezyk, S. P. Reevaluation of Neptunium-Nitric Acid Radiation Chemistry by Multiscale Modeling. *J. Phys. Chem. B* 2016, *120*(49), 12643–12649. DOI: 10.1021/acs.jpcb.6b09683.

[59] Mincher, B. J.; Precek, M.; Mezyk, S. P.; Elias, G.; Martin, L. R.; Paulenova, A. The Redox Chemistry of Neptunium in γ-Irradiated Aqueous Nitric Acid. *Radiochim. Acta* 2013, *101*(4), 259–266. DOI: 10.1524/ract.2013.2013.

[60] Kondé, J.; Distler, P.; John, J.; Švehla, J.; Grüner, B.; Bělčická, Z. Radiation Influencing of the Extraction Properties of the CyMe₄-BTBP and CyMe₄-BTPhen Solvents with FS-13. *Procedia Chem.* 2016, *21*, 174–181. DOI: 10.1016/j.proche.2016.10.025.

[61] Schmidt, H.; Wilden, A.; Modolo, G.; Bosbach, D.; Santiago-Schübel, B.; Hupert, M.; Mincher, B. J.; Mezyk, S. P.; Švehla, J., and Grüner, B., et al. Gamma and Pulsed Electron Radiolysis Studies of CyMe₄BTBP and CyMe₄BTPhen: Identification of Radiolysis Products and Effects on the Hydrometallurgical Separation of Trivalent Actinides and Lanthanides. *Radiat. Phys. Chem.* 2021, *189*, 109696. DOI: 10.1016/j.radphyschem.2021.109696.